Thermal Conductivity and Large Isotope Effect in GaN from First Principles

L. Lindsay, D. A. Broido, and T. L. Reinecke

Phys. Rev. Lett. **109**, 095901 — Published 28 August 2012

DOI: 10.1103/PhysRevLett.109.095901

Thermal conductivity and large isotope effect in GaN from first principles

L. Lindsay[1], D. A. Broido[2], and T. L. Reinecke[1]

[1]Naval Research Laboratory, Washington, D.C. 20375, USA

[2]Department of Physics, Boston College, Chestnut Hill, Massachusetts 02467, USA

Abstract

We present atomistic first principles results for the lattice thermal conductivity of GaN and compare them to those for GaP, GaAs, and GaSb. In GaN we find a large increase to the thermal conductivity with isotopic enrichment, ~65% at room temperature. We show that both the high thermal conductivity and its enhancement with isotopic enrichment in GaN arise from the weak coupling of heat-carrying acoustic phonons with optic phonons. This weak scattering results from stiff atomic bonds and the large Ga to N mass ratio, which give phonons high frequencies and also a pronounced energy gap between acoustic and optic phonons compared to other materials. Rigorous understanding of these features in GaN gives important insights into the interplay between intrinsic phonon-phonon scattering and isotopic scattering in a range of materials.

PACS: 66.70.-f, 63.20.kg, 71.15.-m

Introduction—Gallium nitride (GaN) is a wide band gap semiconductor and a promising candidate for use in optoelectronic devices [1, 2], high-frequency switches [3, 4], and high-power electronics [5]. Thermal management is of critical importance in such devices, especially as typical device sizes continue to decrease. GaN has the attractive feature of an unusually high lattice thermal conductivity, κ_L, with measured room temperature values around 230 $Wm^{-1}K^{-1}$ [6-8]. To date the origin of its high κ_L is not well understood at a quantitative level. Furthermore, increase of its κ_L could lead to better performing and longer-lived electronic devices.

As in other semiconductors, heat in GaN is carried primarily by phonons. The κ_L is limited by intrinsic phonon-phonon scattering around room temperature and higher [9] and by extrinsic scattering due to point defects such as isotopes. Recent work has estimated that the room temperature "isotope effect" given by $P = 100 \times (\kappa_{pure} / \kappa_{natural} - 1)$ is a relatively small 4-15% in GaN [6,10-12]. Here κ_{pure} corresponds to κ_L for isotopically pure GaN and $\kappa_{natural}$ to κ_L with naturally occurring Ga isotope concentrations. Other work has suggested that κ_L of defect-free GaN is much larger than measured values, but that the enhancement comes from removal of vacancies and substitutional defects rather than from isotope enrichment [13, 14].

Reliable determination of κ_L and the effects of different scattering mechanisms depend on an accurate representation of the anharmonic phonon-phonon scattering. In simple models for κ_L, this scattering is often estimated using a mode averaged Gruneisen constant and using parameters adjusted to fit measured data [10, 11]. Such models lack predictive capability. Alternatively, molecular dynamics simulations have been used [15], but these cannot represent quantum mechanical scattering so are of uncertain validity below the Debye temperature of a material (~600K for GaN). In this Letter we employ a first principles approach to definitively

determine κ_L in GaN due to phonon-phonon and isotopic impurity scattering. Unlike previous estimates, our state-of-the-art calculations show that the isotope effect in GaN is very large, ~65% at room temperature, making it comparable to the highest isotope effects observed in diamond (~50%) [16], graphene (60%) [17], and boron nitride nanotubes (~50%) [18]. As a result, we find that the intrinsic upper-limit to κ_L in GaN is around 400 $Wm^{-1}K^{-1}$ at 300K, considerably higher than currently measured κ_L values. These features are a consequence of i) the substantial isotope mixture in Ga, ii) the large energy gap between the acoustic and optic phonons and iii) the high frequency scale of the phonon dispersion in GaN. The latter two points weaken the phonon-phonon scattering and in particular the scattering between the heat carrying acoustic phonons and optic phonons. This leads to higher κ_L and makes isotope scattering relatively more important. We illustrate this effect by comparing the κ_L for GaN with that for GaAs, GaP, and GaSb.

Ab initio thermal transport—We employ a first principles approach to calculate κ_L, which combines an exact numerical solution of the Peierls-Boltzmann transport equation (PBE) with accurate calculations of the harmonic and anharmonic interatomic force constants (IFCs) using density functional theory (DFT) and density functional perturbation theory (DFPT). The absence of accurate values for the anharmonic IFCs has limited quantitative results for κ_L and full understanding of the underlying physics. A similar approach previously used by us has accurately described thermal transport in silicon, germanium and diamond [19, 20]. We consider κ_L limited by intrinsic (three-phonon) and isotope defect scattering processes. The thermal conductivity tensor is:

$$\kappa_{\alpha\beta} = \frac{1}{(2\pi)^3} \sum_j \int (\partial n_\lambda^0 / \partial T) \hbar \omega_\lambda v_{\lambda\alpha} v_{\lambda\beta} \tau_{\lambda\alpha} d\vec{q} \qquad (1)$$

In Eq. 1, ω_λ and $v_{\lambda\alpha} = d\omega_\lambda / dq_\alpha$ are the frequency and α^{th} component of the velocity for a phonon in mode, $\lambda = (\vec{q}, j)$, with wavevector $\vec{q}$ in branch j, n_λ^0 is the Bose distribution function and $\tau_{\lambda\alpha}$ is the phonon lifetime. GaN has a wurtzite structure with underlying hexagonal lattice. We define the layers to be in the x-y plane with the c-axis in the z direction. Then $\kappa_{\alpha\beta}$ is diagonal with one out-of-plane component, κ_{zz}, and two in-plane components, κ_{xx} and κ_{yy}. In principle, for infinite, perfect hexagonal systems $\kappa_{xx}=\kappa_{yy}$, however, isotope scattering introduces in-plane anisotropy. At around room temperature and higher, this anisotropy is only a few percent so we define $\kappa_{in}=(\kappa_{xx}+\kappa_{yy})/2$ and $\kappa_{out}=\kappa_{zz}$ to discuss in-plane and out-of-plane thermal transport.

The linearized PBE is solved using an iterative scheme described in detail previously [19-21]. The intrinsic three-phonon scattering probabilities are:

$$\Gamma^{(\pm)}_{\lambda\lambda'\lambda''} = \frac{\hbar\pi}{4N_0\omega_\lambda\omega_{\lambda'}\omega_{\lambda''}} \begin{Bmatrix} n^0_{\lambda'} - n^0_{\lambda''} \\ n^0_{\lambda'} + n^0_{\lambda''} + 1 \end{Bmatrix} \left|\Phi^{(\pm)}_{\lambda,\pm\lambda',-\lambda''}\right|^2 \delta(\omega_\lambda \pm \omega_{\lambda'} - \omega_{\lambda''}) \qquad (2)$$

$$\Phi_{\lambda\lambda'\lambda''} = \sum_{\kappa}\sum_{l'\kappa'}\sum_{l''\kappa''}\sum_{\alpha\beta\gamma} \Phi_{\alpha\beta\gamma}(0\kappa, l'\kappa', l''\kappa'') \frac{e^{\lambda}_{\alpha\kappa} e^{\lambda'}_{\beta\kappa'} e^{\lambda''}_{\gamma\kappa''}}{\sqrt{\overline{m}_\kappa \overline{m}_{\kappa'} \overline{m}_{\kappa''}}} e^{i\vec{q}'\cdot\vec{R}_{l'}} e^{i\vec{q}''\cdot\vec{R}_{l''}}$$

Here, N_0 is the number of unit cells, and the ± correspond to the three-phonon processes that satisfy conservation of energy and momentum: $\omega_j(\vec{q}) \pm \omega_{j'}(\vec{q}') = \omega_{j''}(\vec{q}'')$ and $\vec{q} \pm \vec{q}' = \vec{q}'' + \vec{K}$, where $\vec{K}$ is a reciprocal lattice vector, which is zero for Normal processes and non-zero for Umklapp processes [9]. Also, $\Phi_{\alpha\beta\gamma}(0\kappa, l'\kappa', l''\kappa'')$ are third-order anharmonic IFCs, $e^{\lambda}_{\alpha\kappa}$ is the α^{th} component of the phonon eigenvector $\hat{e}^{\lambda}_{\kappa}$ for the κ^{th} atom of the unit cell in mode λ, and $\vec{R}_l$ is the lattice vector locating the l^{th} unit cell. The scattering time due to isotopic impurities, τ^{iso}_λ, is given by [22]:

$$1/\tau_{\lambda}^{iso} = \frac{\pi}{2N_0}\omega_{\lambda}^2 \sum_{\kappa} g_{\kappa} \sum_{\lambda'} \left| \hat{e}_{\kappa}^{\lambda} \cdot \hat{e}_{\kappa}^{\lambda'*} \right|^2 \delta(\omega_{\lambda} - \omega_{\lambda'}) \qquad (3)$$

In Eq. 3, $g_{\kappa} = \frac{1}{\overline{m}_{\kappa}^2} \sum_i f_{i\kappa}(m_{i\kappa} - \overline{m}_{\kappa})^2$ is a mass variance parameter with $f_{i\kappa}$ and $m_{i\kappa}$ being the concentration and mass of the i^{th} isotope of the κ^{th} atom, and $\overline{m}_{\kappa}$ being the average mass. For gallium (60.11% ^{69}Ga and 39.89% ^{71}Ga), $g_{Ga} = 1.97 \times 10^{-4}$, while for N, the isotope variation is negligible, $g_N = 0$.

The formalism described above requires harmonic IFCs to calculate phonon frequencies and eigenvectors from diagonalization of the dynamical matrix. It also requires the $\Phi_{\alpha\beta\gamma}(0\kappa, l'\kappa', l''\kappa'')$ to allow calculation of the matrix elements for phonon-phonon scattering in Eq. 2. These IFCs were calculated within the framework of DFT/DFPT using norm-conserving pseudopotentials in the local density approximation (LDA) with the Quantum Espresso package [23]. The ground state configuration for the wurtzite lattice was determined by varying the in-plane, *a*, and out-of-plane, *c*, lattice constants to find the minimum energy, and the internal parameter, *u*, was chosen so that the residual Hellman-Feynman forces on the atoms were zero. We find lattice constants that are 1.8% less than experiment (a_{exp}=3.190Å, c_{exp}=5.189Å, u_{exp}=0.377 [24]). This is consistent with a known shortcoming of LDA approaches, which overbind atoms by 1-2% [25]. Inclusion of zero-point and finite temperature atomic motion [26] into LDA results gives an increase of only about 0.2% to the zero temperature lattice constants. Since the values of lattice constants affect vibrational properties, it is important to correct for this limitation of LDA calculations. Here we give results using harmonic and anharmonic IFCs calculated for the following two choices: Set 1) *a*=3.138Å, *c*=5.109Å, and *u*=0.377 determined by energy minimization with a 0.2% increase, and Set 2) *a*=3.164Å, *c*=5.150Å, and *u*=0.377

determined by energy minimization with an increase of 1.0% in the lattice constants, more consistent with measured values. Figure 1 shows the calculated phonon dispersions for wurtzite GaN using Set 1 (dashed lines) and Set 2 (solid lines) compared with experimental inelastic X-ray data (circles) in the high-symmetry directions [27]. For the low frequency acoustic branches there is little difference between the two sets. However, the high lying optic phonon branches are shifted to lower frequencies with the larger lattice constants. These shifts are consistent with the *ab initio* calculations in Ref. 27 which scaled the LDA phonon dispersion by 0.97 to fit experiment better.

To determine the anharmonic IFCs, we used a real-space approach similar to that of Ref. 28. Pairs of atoms were systematically perturbed from the ground state configuration of a large supercell. The resulting Hellman-Feynman forces on all the atoms were calculated via Γ-point self-consistent calculations for a number of different perturbations to obtain numerical derivatives of the forces, which gave the anharmonic IFCs for three-phonon scattering. For wurtzite GaN we used 108 atom supercells and calculated anharmonic IFCs involving a unit cell atom and its 27 nearest neighbors (4^{th} neighbor shell). We also considered the less common metastable zinc blende phase of GaN for which we used 216 atom supercells and calculated anharmonic IFCs for a unit cell atom and its 29 nearest neighbors (3^{rd} neighbor shell). In principle anharmonic terms from all atomic interactions can enter the scattering matrix elements (Eq. 2) and longer range terms may be important in polar semiconductors with Coulomb interactions. To test the effect of including only the nearest neighbors described above we calculated κ_L for Si, Ge, GaAs, and GaP using anharmonic IFCs obtained from two approaches: 1) the real-space approach described above, and 2) a reciprocal-space DFPT approach [19, 20, 29] which included short-ranged interactions out to seventh nearest neighbors and long-range

Coulomb interactions. We find less than 3% difference in the corresponding κ_L values from the two approaches.

Results—Figure 2 shows $\kappa_L(T)$ of wurtzite GaN between 100K and 500K. The circles and triangles correspond to the measured κ_L of Ref. 6 and Ref. 7, respectively. All curves were determined using the Set 2 lattice constants, which gave the best fit to the experimental data in Fig. 1. The black curves are the calculated κ_L for isotopically pure GaN, κ_{pure}, in which all Ga atoms are ^{69}Ga. The red curves are the calculated κ_L for naturally occurring Ga isotope concentrations, $\kappa_{natural}$. The solid curves correspond to κ_{in} (in-plane transport) and the dashed curves correspond to κ_{out} (transport along the *c* axis).

The phonon-phonon scattering rates increase with temperature while the phonon-isotope scattering rates are temperature independent (see Eq. 3). Thus starting from 500K, with decreasing *T* phonon-phonon scattering becomes weaker causing κ_L to rise and making isotope impurity scattering more important. This is evident from the increasing percent isotope effect, *P*, and seen in the separation between the black and red curves.

The calculated curves for $\kappa_{natural}$ are in good agreement with the experimental data [6, 7] and have room temperature values: κ_{in}=242Wm^{-1}K^{-1} and κ_{out}=239Wm^{-1}K^{-1}. We have estimated the effects of other point defect scattering such as from N isotopic impurities, Ga vacancies, and Oxygen (O) substitutions representing them by the simple mass-difference scattering rates from Eq. 3 and taking the concentrations reported in Ref. 7 (Ga vacancies~10^{18}/cm^{-3} and O impurities~10^{20}/cm^{-3}). We find that including N isotopic impurities and O substitutions have almost no effect on $\kappa_{natural}$ at room temperature and including Ga vacancies lowers $\kappa_{natural}$ around 2.5%.

The calculated curves for κ_{pure} are well above the measured data and represent the intrinsic upper-limit for κ_L in GaN. At room temperature, κ_{in}=401Wm^{-1}K^{-1} and κ_{out}=385Wm^{-1}K^{-1} corresponding to P~60-65% for wurtzite GaN. With decreasing temperature, this isotope effect increases, nearing 100% at T=100K. At even lower T, sample size begins to play a role and the interplay between phonon-phonon and phonon-isotope scattering with that from sample boundaries causes a peak in κ_L (not shown). We have included phonon boundary scattering here using an empirical relaxation time [9], $\tau_\lambda^B = L/|\vec{v}_\lambda|$, with L=1mm as a measure of the sample size consistent with experiment. For all cases κ_L peaks around T=30K with κ_{pure}=22,000Wm^{-1}K^{-1} being almost seven times larger than $\kappa_{natural}$=3300Wm^{-1}K^{-1} (P~600%).

To understand the above findings better, we have calculated the κ_L for zinc blende GaX compounds with X=N, P, As and Sb spanning a wide range of properties, given in Table I. The mass variance parameter for antimony, (57.21% ^{121}Sb and 42.79% ^{123}Sb), is $g_{Sb} = 6.59 \times 10^{-5}$, while the negligible isotope mixtures for phosphorous (P) and arsenic (As) give g_P=g_{As}=0. Figure 3 shows P .vs. T for wurtzite GaN and zinc blende GaN, GaAs, GaSb, and GaP. The smallest P values occur for GaAs, with P=4.4% at T=300K. Our calculated $\kappa_{natural}$ and P for GaAs are in good agreement with κ_L measurements made for isotopically enriched GaAs crystals (99.4% ^{71}Ga and 0.6% ^{69}Ga) which found a P=5% at 300K [30]. The P for the GaN polymorphs lie well above those for the other zinc blende compounds.

One might naively assume that GaSb would have the largest enhancement to κ_L with isotopic enrichment because of the larger isotope mixture. However, for given isotope mixture, it is the interplay between the phonon-phonon scattering and the phonon-isotope scattering that determines P. Comparing successively GaAs, GaSb, GaP, and GaN (Table I) we find that the phonon-phonon scattering is weakened by a) increasing mass difference between Ga and anion

atoms, which produces a larger acoustic-optic frequency gap, as seen in Fig 1 for GaN, and by b) increasing atomic bond stiffness and decreasing mass of constituent atoms, which raise the entire phonon spectrum to higher frequencies. Consider point b) first. Higher overall phonon frequencies reduce the phonon populations of all modes and also reduce the phase space for three-phonon scattering [31], thereby decreasing the phonon-phonon scattering rates. We note that increasing bond stiffness also increases the anharmonic IFCs thereby enhancing the phonon-phonon scattering matrix elements (Eq. 2), but the stronger influence from the higher phonon frequencies ultimately leads to reduced scattering rates with increasing bond stiffness in materials such as GaN. We further verified the importance of the frequency scale in determining κ_L and P by scaling down the full frequency spectrum in wurtzite GaN. The resulting increased phonon-phonon scattering rates significantly lowered κ_L and P. Reduced acoustic phonon velocities also lowered κ_L.

Consider now point a). Optic phonons play a critical role in determining κ_L of GaN. Although optic phonons do not significantly contribute directly to a thermal current, they do provide important scattering channels for the heat-carrying acoustic phonons as has been pointed out recently for silicon [19], diamond [20], and lead telluride [32-34]. The extremely large frequency gap in GaN has a dramatic effect on κ_L and P because it strongly restricts three-phonon scattering between acoustic and optic phonons [31] through the energy conservation seen in Eq. 2 [35, 36]. On the other hand, the isotopic impurity scattering is not much affected by the gap. This point is highlighted by comparison of GaN with silicon. Si has lighter unit cell mass, higher acoustic phonon frequency scale and acoustic velocities, smaller anharmonic IFCs and similar isotope scattering (for naturally occuring Si) compared to GaN. These features suggest that Si should have larger κ_L and P compared to GaN. However, Si has no acoustic-optic

frequency gap. Thus, we find that the calculated κ_{pure} for Si at room temperature ($155 Wm^{-1}K^{-1}$) is nearly three times smaller than κ_{pure} for GaN and the calculated P (7.6%) for Si is almost nine times smaller than that for GaN [37, 38]. These differences stem primarily from the large frequency gap in GaN and the much weaker acoustic-optic phonon scattering that results.

Summary and Conclusions—We have examined the lattice thermal conductivity, κ_L, of GaN and its dependence on isotopes using a microscopic, first principles approach. The calculated κ_L with naturally occurring isotope concentration is in good agreement with measured values over a broad temperature range, and the increase in κ_L with isotopic enrichment (~65% at room temperature) is comparable to that of the highest observed enhancements in diamond, graphene, and boron nitride nanotubes. We find that the large κ_L and isotope effect in GaN result from the large Ga isotope mixture, the mass difference between constituent atoms, the light N mass and strong bond stiffness. The resulting large frequency gap between the acoustic and optic phonon branches and the high phonon frequency scale lead to unusually weak anharmonic phonon-phonon scattering. This interpretation is validated by comparison with GaAs, GaSb, and GaP. The rigorous understanding of phonon-phonon scattering and κ_L presented here for GaN gives important insights into the origin of thermal conductivity and the role of isotopes in other systems.

Acknowledgements: This work was supported in part by ONR and DARPA (L.L. and T.L.R.). L.L. acknowledges support from the NRC/NRL Research Associateship Program. D.A.B acknowledges support from the National Science Foundation under Grant No. 1066634 and from the S3TEC, an Energy Frontier Research Center funded by the US Department of Energy, Office of Science, Office of Basic Energy Sciences under Award No. DE-FG02-09ER46577.

References

[1] S. N. Mohammad, A. A. Salvador, and H. Morkoç, Proc. of the IEEE **83**, 1306 (1995).

[2] K. Chung, C.-H. Lee, and G.-C. Yi, Science **330**, 655 (2010).

[3] K. Shenai, K. Shah, and H. Xing, Proc. of the IEEE NAECON Conf., 317 (2010).

[4] S. Dargahi, P. Valizadeh, and S. S. Williamson, Veh. Power and Prop. Conf. IEEE, 1 (2011).

[5] M. A. Briere, Power Elec. Europe **7**, 29 (2008).

[6] G. A. Slack, L. J. Schowalter, D. Morelli, and J. A. Freitas, J. of Crystal Growth **246**, 287 (2002).

[7] A. Jeżowski, P. Stachowiak, T. Plackowski, T. Suski, S. Krukowski, M. Boćkowski, I. Grzegory, B. Danilchenko, and T. Paszkiewicz, Phys. Stat. Sol. (b) **240**, 447 (2003).

[8] C. Mion, J. F. Muth, E. A. Preble, and D. Hanser, Appl. Phys. Lett. **89**, 092123 (2006).

[9] J. M. Ziman, *Electrons and Phonons* (Oxford University Press, London, 1960).

[10] A. AlShaikhi, S. Barman, and G. P. Srivastava, Phys. Rev. B **81**, 195320 (2010).

[11] X.-G. Yu and X.-G. Liang, Diamond and Rel. Mat. **16**, 1711 (2007).

[12] D. T. Morelli, J. P. Heremans, and G. A. Slack, Phys. Rev. B **66**, 195304 (2002).

[13] A. Witek, Diamond and Rel. Mat. **7**, 962 (1998).

[14] R. Berman, Diamond and Rel. Mat. **8**, 2016 (1999).

[15] X. W. Zhou, S. Aubry, R. E. Jones, A. Greenstein, and P. K . Schelling, Phys. Rev. B **79**, 115201 (2009).

[16] T. R. Anthony, W. F. Banholzer, J. F. Fleischer, L. Wei, P. K. Kuo, R. L. Thomas, and R. W. Pryor, Phys. Rev. B **42**, 1104 (1990).

[17] S. Chen, Q. Wu, C. Mishra, J. Kang, H. Zhang, K. Cho, W. Cai, A. A. Balandin, and R. S. Ruoff, Nature Mat. **11**, 203 (2012).

[18] C.W. Chang, A.M. Fennimore, A. Afanasiev, D. Okawa, T. Ikuno, H. Garcia, Deyu Li, A. Majumdar, and A. Zettl, Phys. Rev. Lett. **97**, 085901 (2006).

[19] D. A. Broido, M. Malorny, G. Birner, N. Mingo and D. A. Stewart, Appl. Phys. Lett. **91**, 231922 (2007).

[20] A. Ward, D. A. Broido, D. A. Stewart and G. Deinzer, Phys. Rev. B **80**, 125203 (2009).

[21] M. Omini and A. Sparavigna, Phys. Rev. B **53**, 9064 (1996).

[22] S. I. Tamura, Phys. Rev. B **30**, 849 (1984).

[23] S. Baroni et al., http://www.quantum-espresso.org.

[24] H. Schulz and K. H. Thiemann, Sol. State Comm. **23**, 815 (1977).

[25] P. Haas, F. Tran, and P. Blaha, Phys. Rev. B **79**, 085104 (2009).

[26] P. B. Allen, Phil. Mag. B **70**, 527 (1994).

[27] T. Ruf, J. Serrano, M. Cardona, P. Pavone, M. Pabst, M. Krisch, M. D'Astuto, T. Suski, I Grzegory, and M. Leszczynski, Phys. Rev. Lett. **86**, 906 (2001).

[28] K. Esfarjani and H. T. Stokes, Physical Review B 77, 144112 (2008).

[29] G. Deinzer, G. Birner and D. Strauch, Phys. Rev. B **67**, 144304 (2003).

[30] A. V. Inyushkin, A. N. Taldenkov, A. Yu Yakubovsky, A.V. Markov, L Moreno-Garsia and B. N. Sharonov Semicond. Sci. Technol. **18**, 685 (2003).

[31] L. Lindsay and D. A. Broido, J. Phys.: Con. Mat. **20**, 165209 (2008).

[32] J. An, A. Subedi, and D. J. Singh, Solid State Comm. **148**, 417 (2008).

[33] O. Delaire, J. Ma, K. Marty, A. F. May, M. A. McGuire, M.-H. Du, D. J. Singh, A. Podlesnyak, G. Ehlers, M. D. Lumsden, and B. C. Sales, Nature Mat. **10**, 614 (2011).

[34] Z. Tian, J. Garg, K. Esfarjani, T. Shiga, J. Shiomi, and G. Chen, Phys. Rev. B **85**, 184303 (2012).

[35] We note that wurtzite GaN has three mid-frequency optic phonon branches, which play a role in determining κ_L The two lower optic branches are quite dispersive and contribute significantly to κ_L. Artificial removal of the highest mid-frequency optic branch further reduces the acoustic-optic phonon scattering and enhances κ_L.

[36] This point is further supported by the 10% higher calculated room temperature $\kappa_{natural}$ and κ_{pure} obtained using the Set 1 lattice constants for GaN, which give higher optic mode frequencies. Note that the isotope effect predicted by Set 1and Set 2 lattice constants is almost the same.

[37] Both calculated values for Si are in good agreement the measured values in Ref. 38.

[38] A. V. Inyushkin, A. N. Taldenkov, A. M. Gibin, A. V. Gusev and H.–J. Pohl, Phys. Stat. Sol. (c), 1, 2995 (2004).

Table I. Calculated mass mismatch, frequency gap between acoustic and highest optic phonon branches, LA phonon frequency at the X (M) point for zinc blende (wurtzite) structure, $\kappa_{natural}$ at T=300K, and percent isotope effect (P) for Ga-based semiconductors.

	$\left\|1-\frac{\overline{m}_{Ga}}{\overline{m}_{anion}}\right\|$	*frequency gap* (THz)	ω_{LA} (THz)	$\kappa_{natural}$ ($Wm^{-1}K^{-1}$)	P
GaAs	0.07	0	6.70	52	4
GaSb	0.43	0.75	4.83	42	8
GaP	1.25	2.48	7.70	123	14
cubic GaN	3.98	6.01	10.6	215	68
wurtzite GaN	3.98	6.11	9.34	242	66

Table I

Figure Captions

Figure 1 Calculated phonon dispersion for wurtzite GaN in high symmetry directions with Set 1 (dashed lines) and Set 2 (solid lines) lattice constants described in the text. The hollow circles correspond to experimental data determined by inelastic X-ray scattering [27].

Figure 2 Calculated thermal conductivity .vs. temperature for naturally occurring ($\kappa_{natural}$, two lower red lines) and isotopically pure (κ_{pure}, two upper black lines) wurtzite GaN given by Set 2 lattice constants (described in text). Solid lines correspond to κ_{in} and dashed lines to κ_{out}. The symbols correspond to experimental data from Ref. 6 (circles) and Ref. 7 (triangles).

Figure 3 Calculated percent isotope effect, P, .vs. temperature for GaAs (blue (lowest)), GaSb (green (lower)), GaP (red (middle)), wurtzite GaN (dashed black), zinc blende GaN (solid black (highest)).

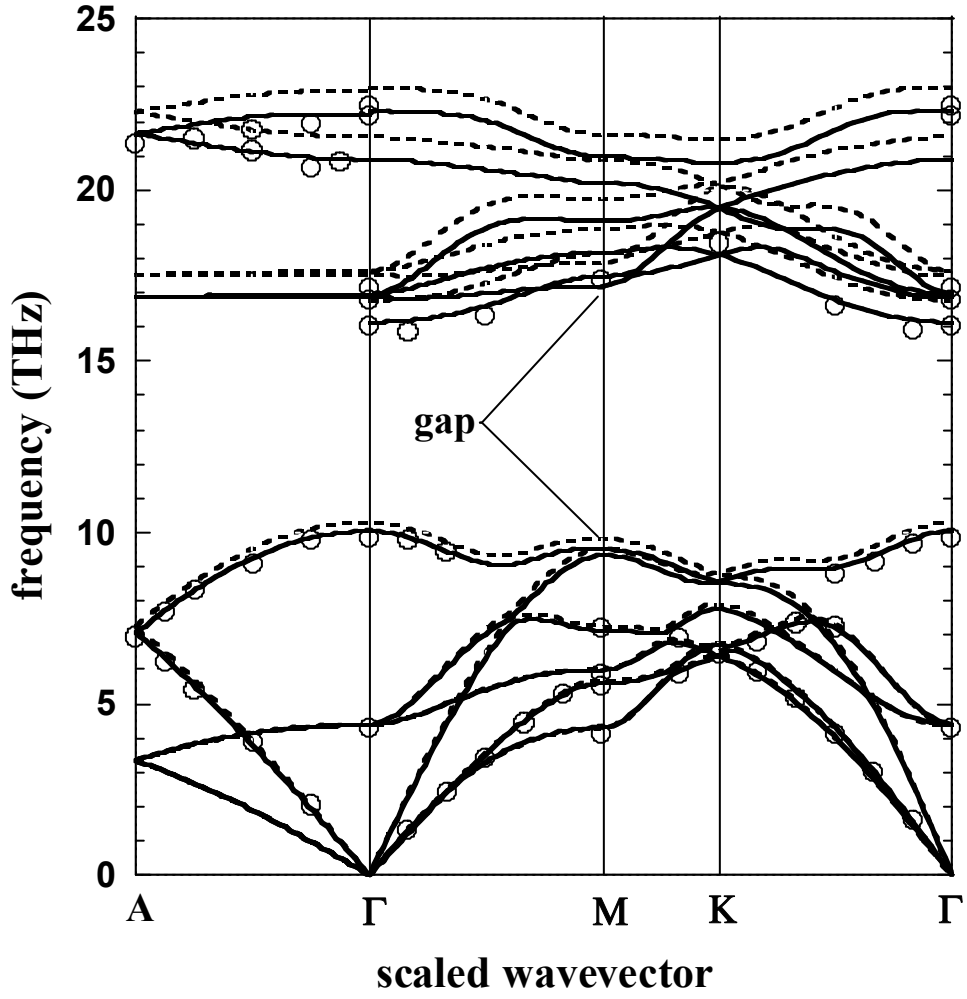

Figure 1

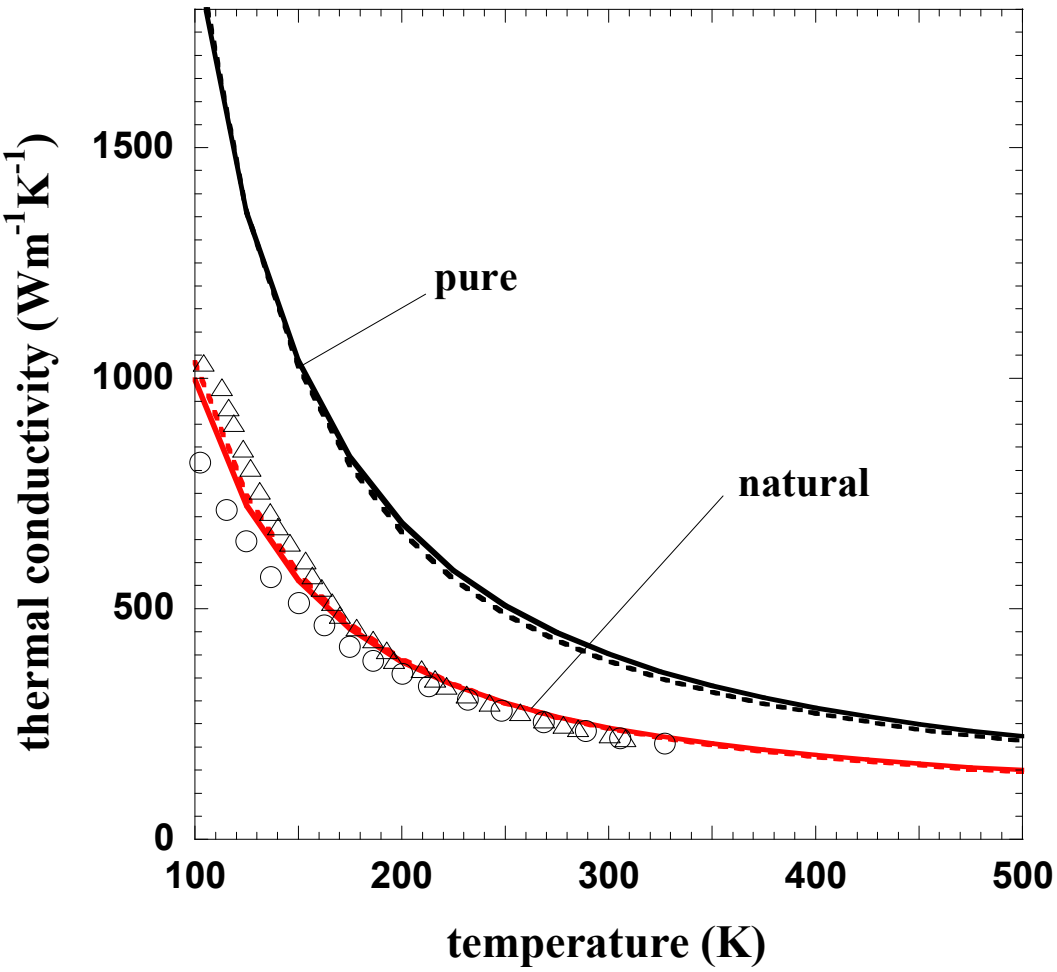
thermal conductivity (Wm-1K-1)
1500
1000
500
0
100
200
300
400
500
temperature (K)
pure
natural

Figure 2

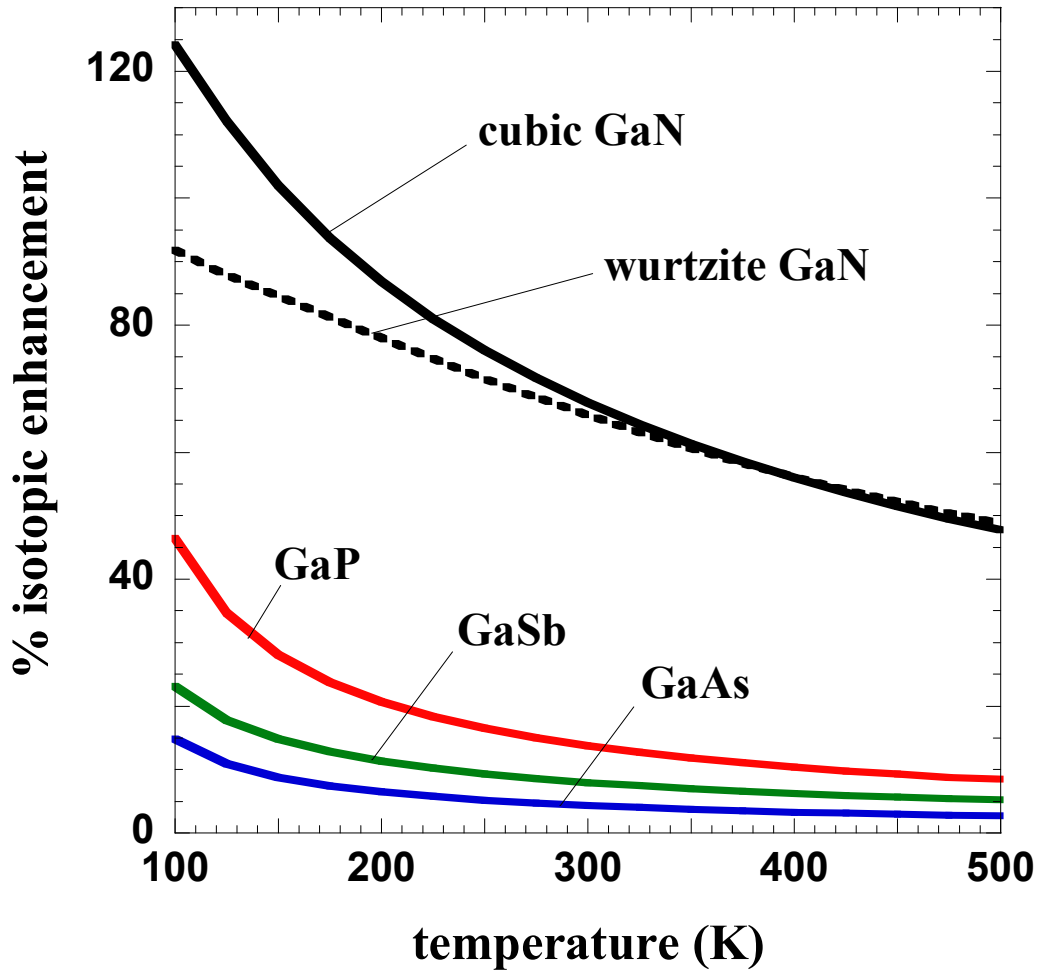
120
80
40
0
% isotopic enhancement
cubic GaN
wurtzite GaN
GaP
GaSb
GaAs
100
200
300
400
500
temperature (K)

Figure 3